



Contents lists available at ScienceDirect

## Bioorganic &amp; Medicinal Chemistry Letters

journal homepage: [www.elsevier.com/locate/bmcl](http://www.elsevier.com/locate/bmcl)

## New C<sup>4</sup>- and C<sup>1</sup>-derivatives of furo[3,4-c]pyridine-3-ones and related compounds: Evidence for site-specific inhibition of the constitutive proteasome and its immunoisofom



Anna Hovhannisyann<sup>c,†</sup>, The Hien Pham<sup>a,b,†</sup>, Dominique Bouvier<sup>d,†</sup>, Alexander Piroyan<sup>c</sup>, Laure Dufau<sup>a,b</sup>, Lixian Qin<sup>a,b</sup>, Yan Cheng<sup>a,b</sup>, Gagik Melikyan<sup>c</sup>, Michèle Reboud-Ravaux<sup>a,b</sup>, Michelle Bouvier-Durand<sup>a,b,\*</sup>

<sup>a</sup> Sorbonne Universités, UPMC Univ Paris 06, UMR 8256, ERL U1164, B2A, Biological Adaptation and Ageing, Integrated Cellular Ageing and Inflammation, Molecular & Functional Enzymology, Case 256, 7 Quai St Bernard, F-75005 Paris, France

<sup>b</sup> CNRS, UMR 8256, B2A, Biological Adaptation and Ageing, F-75005 Paris, France

<sup>c</sup> Department of Organic Chemistry, Yerevan State University, A. Manoogian Str. 1, 0025 Yerevan, Armenia

<sup>d</sup> Sorbonne Universités, UPMC Univ Paris 06, Atelier de Bioinformatique, Case courrier 1202, 4 Place Jussieu, F 75252 Paris Cedex 05, France

## ARTICLE INFO

## Article history:

Received 25 November 2013

Revised 22 January 2014

Accepted 23 January 2014

Available online 3 February 2014

## Keywords:

Furo[3,4-c]pyridine-3-ones

Furo- and thieno[2,3-d]pyrimidine-4-ones

CT-L

T-L and PA proteolytic activities

Constitutive c20S proteasome

Immunoproteasome i20S

In silico docking

## ABSTRACT

A set of 18 new C<sup>4</sup> and C<sup>1</sup> derivatives of nor-cerpegin (1,1-dimethyl furo[3,4-c]pyridine-3-one), 6 model compounds ( $\gamma$ - and  $\delta$ -lactones) and 20 furo- or thieno[2,3-d]-pyrimidine-4-one related compounds were designed and synthesized. Each compound was assayed for inhibition of CT-L, T-L and PA proteolytic activities of 20S constitutive proteasome (c20S). Most performant compounds were also assayed on 20S immunoproteasome (i20S). Compound **10** with a benzylamino group at C<sup>4</sup> and dimethylated at C<sup>1</sup> of the furopyridine ring was the most efficient PA site-specific inhibitor of the c20S (IC<sub>50</sub><sup>cPA</sup> of 600 nM) without noticeable inhibition of the i20S PA site (iPA). In silico docking assays for **10** at the iPA catalytic site revealed the absence of poses normally observed for this compound and related ones at the constitutive PA site (cPA). The thieno[2,3-d]pyrimidine-4-one **40** was T-L site-specific with a mild inhibition of both c20S and i20S in vitro (IC<sub>50</sub><sup>CT-L</sup> of 9.9  $\mu$ M and IC<sub>50</sub><sup>T-L</sup> of 6.7  $\mu$ M). In silico docking assays of **40** at T-L sites of c20S and i20S revealed almost identical first rank poses in the two types of sites with no possibility left for nucleophilic attack by Thr1 as observed for the fused furopyridine-3-one **10**.

© 2014 Elsevier Ltd. All rights reserved.

In a preceding article,<sup>1</sup> we reported on derivatives of 1,1,5-trimethylfuro[3,4-c]pyridine-3,4-dione (cerpegin, a pyridinone-fused  $\gamma$ -lactone) and their use as inhibitors of 20S proteasome, with initial optimization when compared to the series originally described.<sup>2</sup> Our present work takes advantage of interesting properties of the identified lead compounds as selective inhibitors of the post-acid activity of mammalian constitutive 20S proteasomes. A search for new analogs with optimized

inhibitory power and preserved selectivity was conducted. This work also takes advantage of the knowledge of several classes of inhibitors of the catalytic core (20S or CP) already described for the constitutive 26S proteasome<sup>3–6</sup> and more recently, for the immunoproteasome (reviewed in Ref. 7) (c20S and i20S, respectively).

In eukaryotic cells, 26S proteasomes are essential proteolytic components of the general ubiquitin-proteasome pathway (UPS), with a dependency for energy and ubiquitin.<sup>3–6</sup> Many cellular functions (cell cycle progression,<sup>8</sup> apoptosis,<sup>9</sup> transcription,<sup>10</sup> checkpoint control of DNA damage and DNA repair,<sup>10</sup> degradation of abnormal proteins by the ERAD (Endoplasmic Reticulum-Associated Degradation)<sup>11</sup> pathway, are dependent on the proteasomal action to specifically cleave key protein substrates into small peptides. In mammalian lymphocytes and monocytes, c20S also shapes a part of the peptides loaded on the major histocompatibility complex class I (MHC-I).<sup>3–5,7</sup> In all mammalian cells, another panel of MHC-I peptides is shaped by the immunoproteasome after induction by cytokines.<sup>12</sup>

**Abbreviations:** DMF DMA, dimethylformamide dimethylacetal; DMSO, dimethylsulfoxide; c20S, 20S constitutive proteasome catalytic core; i20S, immunoproteasome catalytic core; CT-L, chymotrypsin-like; T-L, trypsin-like; PA, post-acid or caspase-like; AMC, 7-amino-4-methyl-coumarin;  $\beta$ -NA,  $\beta$ -naphthylamide; CPK, Corey Pauling Koltun; PDB, protein data bank.

\* Corresponding author. Tel.: +33 1 44 27 59 62; fax: +33 1 44 27 51 40.

**E-mail addresses:** [annahovh@gmail.com](mailto:annahovh@gmail.com) (A. Hovhannisyann), [bsthehien@yahoo.com](mailto:bsthehien@yahoo.com) (T.H. Pham), [dbouvier@snv.jussieu.fr](mailto:dbouvier@snv.jussieu.fr) (D. Bouvier), [aleksandr.piroyan@gmail.com](mailto:aleksandr.piroyan@gmail.com) (A. Piroyan), [dufaulaure@yahoo.fr](mailto:dufaulaure@yahoo.fr) (L. Dufau), [lixian.qin@free.fr](mailto:lixian.qin@free.fr) (L. Qin), [cyan86520@hotmail.com](mailto:cyan86520@hotmail.com) (Y. Cheng), [acect@yahoo.com](mailto:acect@yahoo.com) (G. Melikyan), [Michele.Reboud@upmc.fr](mailto:Michele.Reboud@upmc.fr) (M. Reboud-Ravaux), [mbouvier@snv.jussieu.fr](mailto:mbouvier@snv.jussieu.fr) (M. Bouvier-Durand).

<sup>†</sup> These authors contributed equally to this work.

<http://dx.doi.org/10.1016/j.bmcl.2014.01.072>

0960-894X/© 2014 Elsevier Ltd. All rights reserved.

The CP particles of c20S and i20S form a similar cylindrical structure, each comprising four stacked heptameric rings ( $\alpha 1-7$   $\beta 1-7$   $\alpha 1-7$ ). The different proteolytic activities of c20S or i20S are confined to the two identical inner  $\beta$  rings. In a single  $\beta$  ring, only the  $\beta 1$ ,  $\beta 2$  and  $\beta 5$  subunits possess a proteolytic activity, the so-called caspase-like (C-L or PA), trypsin-like (T-L) and chymotrypsin-like (CT-L) activity, respectively.<sup>3–5,13–17</sup> Whatever the nature of the catalytic particle (c20S or i20S), each type of proteolytic site possesses a threonine residue at position 1 capable of nucleophilic attack on the substrates. However, specificity of the respective sites ( $\beta 1$ ,  $\beta 2$  and  $\beta 5$ ) can be distinguished in vitro by placing acidic, basic or hydrophobic residues at the C-terminal end of fluorogenic substrates. Despite small variations in the amino acid sequences of the respective catalytic subunits of i20S,  $\beta 1i$  (LMP2),  $\beta 2i$  (MECL-1) and  $\beta 5i$  (LMP7), the same substrates can be used as those for c20S to evaluate the respective activities.  $\beta 5i$  subunits have been recently reported as key regulators of cytokine production with selective inhibition by the epoxyketone PR-957 and therapeutic applications for experimental arthritis.<sup>18</sup> A recent X-ray study<sup>7</sup> of this compound bound to the mouse i20S or c20S crystal structures showed the absence of conformational changes in the S1 specificity pocket of  $\beta 5i$  site, explaining the selectivity of PR-957 for  $\beta 5i$ . Site-specific proteasome inhibitors are not confined to  $\beta 5$  sites since  $\beta 1$  ones have been shown to be the specific targets of IPSI-001<sup>19</sup> and LMP2-ek<sup>19</sup> in the case of i20S. Both  $\beta 1c$  and  $\beta 1i$  sites are inhibited by peptido-epoxyketones YU-102,<sup>20</sup> NC-001<sup>21</sup> and LU-102.<sup>22</sup> As regards  $\beta 2$  sites, NC-022 is a specific inhibitor of T-L activity.<sup>23</sup>

Cell cycle progression and apoptosis induction are the cellular functions best known for their susceptibility to proteasome inhibition. The dipeptide boronate bortezomib (or Velcade<sup>®</sup>, initially PS341) was the only one that came to therapeutic step among the first generation of inhibitors. Successful treatments with this molecule were reported in 2003 on multiple myeloma and then in 2006 on relapsed mantle cell lymphoma. Because of drastic side effects and the appearance of resistant cells, a second generation of inhibitors has been developed. Two other peptide-boronates, CEP-18770 and MLN9708, the tetrapeptide epoxyketone carfilzomib and the  $\beta$ -lactone salinosporamide A, have been the subject of intensive clinical studies.<sup>24</sup> Carfilzomib (Kyprolis or PR-171) has been recently approved by FDA for the treatment of multiple myeloma.<sup>25</sup> Salinosporamide A (SalA, NPI 0052 or marizomib) belongs to a large family of natural compounds (omuralide,  $\beta$ -lactosin A, reviewed in Ref. 6) and is a highly potent inhibitor of c20S with a  $\beta$ -lactone working as a pharmacophore. SalA has been retained in this study as a reference  $\beta$ -lactone<sup>24</sup> as well as cerpegin derivatives possessing a  $\gamma$ -lactone moiety.<sup>1,2</sup> These two categories of lactones are covalent inhibitors and, together with peptide mimetics, they represent a large class of molecules known to target the 20S catalytic core.<sup>26–28</sup> Non-covalent inhibitors have been more recently developed<sup>28</sup> including hydroxyurea (HU) compounds,<sup>29</sup> oxadiazoles,<sup>30</sup> and peptidic derivatives.<sup>31–34</sup>

The aim of the present study was to synthesize new molecules bearing a  $\gamma$ -lactone moiety on the model of cerpegin and derivatives<sup>1,2,35</sup> with substitutions at the C<sup>4</sup> of the furo[3,4-*c*]pyridine-3-one skeleton. Optimization of their inhibitory power towards c20S fractions in vitro was first investigated and the most interesting compounds from this approach were selected for testing their efficiency on i20S fractions. Furthermore, calpain 1 and cathepsin B activities were assayed in order to check the specificity of proteasome inhibition. Whole cell assays were also conducted to measure intracellular proteasome inhibition and to evaluate cytotoxicity. New furo- and thieno[2,3-*d*]pyrimidine-4-one compounds were also synthesized and assayed for their aptitude to inhibit c20S proteasome. For the most potent compounds identified as inhibitors of c20S or i20S, the possible mechanisms of binding were

investigated by in silico docking. Previous studies from our group have suggested a covalent mechanism of inhibition associated with a unique mode of binding of cerpegin-derived  $\gamma$ -lactones to the bovine  $\beta 1c$  active site.<sup>1,2</sup>

The general structures of the molecules synthesized and evaluated in this study are presented in Figure 1(B–E) whereas reference compounds are presented in Figure 1A. The  $\beta$ -lactone of SalA (Fig. 1A, top) is attacked by the nucleophilic Thr1 and this leads to formation of a highly stable acyl-enzyme.<sup>24</sup> The  $\gamma$ -lactone ring of cerpegin (Fig. 1A, bottom) is also susceptible to nucleophilic attack by Thr1 and we have recently reported kinetic results showing covalent proteasome inhibition by a cerpegin derivative.<sup>2</sup> Furthermore, cerpegin derivatives substituted at N<sup>5</sup> or at N<sup>5</sup> and C<sup>1</sup> showed selectivity towards the post-acid activity (IC<sub>50</sub> 2–10  $\mu$ M).<sup>1,2</sup> Based on these results, new series of molecules have been designed to retain the  $\gamma$ -lactone of the fused furo[3,4-*c*]pyridine ring of cerpegin. C<sup>4</sup>- and C<sup>1</sup>-substituted furo[3,4-*c*]pyridine-3-one derivatives with main variations of the functional groups at C<sup>4</sup> position (labeled R in Fig. 1B) were synthesized. These R groups were mainly chosen on the basis of our previous results where they appeared as efficient N<sup>5</sup> substituents.<sup>1,2</sup>

Some other  $\gamma$ -lactones not fused to a pyridine ring were also designed and prepared (Fig. 1C, 19–22), together with two pyridine-fused  $\delta$ -lactones (Fig. 1C, 23 and 24) as model compounds to evaluate the effects of the lactone environment.

The role of carbonyl-derived chemical groups other than  $\gamma$ -lactones, placed in various heterocyclic environments (fused furo- and thienopyrimidine-4-ones), was also investigated (Fig. 1D and E).

The aforementioned C<sup>4</sup>- and C<sup>1</sup>-substituted furo[3,4-*c*]pyridine-3-one derivatives (Fig. 1B) were synthesized as outlined in Scheme 1A and B. Scheme 1A sums up steps for the synthesis of compounds of series IV and VIII (1–4), III and VI (7–18). Compounds XI (5, 6) were synthesized according to Scheme 1B. The unfused  $\gamma$ -lactone models 19, 20, 21, 22 were synthesized as previously reported (19, 20,<sup>35,36</sup> 21,<sup>2</sup> 22<sup>37</sup>). The pyridinone-fused  $\delta$ -lactones 23 and 24 were prepared as mentioned in<sup>38</sup> for 23, and according to Scheme 1C for 24.

The most convenient way of synthesis of nor-cerpegin (1,1-dimethyl furo[3,4-*c*]pyridine-3,4-dione) (compound 1 in series IV) was based on the use of easily accessible carbonitriles I reacting with DMF DMA (Scheme 1A, i). Further cyclization in a AcOH/HCl (3:1) mixture of dimethylaminovinyl derivatives II led to high yields of product IV (1) (Scheme 1A, iii). The same steps were used to produce compound 2.

Primary 4-amino derivatives III (7–9) were obtained in high yields by reacting intermediates II in 20% ammonia (Scheme 1A, ii). For the synthesis of 4-substituted amino furo pyridines VI (10–14), the 4-chloro-derivative V obtained from compounds IV (7) and PCl<sub>5</sub> interaction at 130–150 °C during 15–20 min was used (Scheme 1A, iv). On a first way to compounds VI (10–14), primary amines were reacted with V under reflux in xylene (Scheme 1A, v, a), whereas secondary amines were reacted in boiling DMF (Scheme 1A, v, b), and aromatic amines were reacted in AcOH (Scheme 1A, v, c). All reactants are summed up in Supplementary Table S1. On a second way, several substituted amino derivatives VI (15–18) with a side-chain hydroxyl group were synthesized from the primary amine III (7) through reaction with oxiranes (Scheme 1A, vi). The presence of a hydroxyl group on a side-chain could lead to significant improvement of the binding affinity to proteasome active sites, as already reported in our investigations on cerpegin N<sup>5</sup> derivatives.<sup>2</sup>

For comparison purposes, 4-thioxo VIII (3, 4) (Scheme 1A) and 4-methyl XI (5, 6) (Scheme 1B) derivatives were synthesized. The 4-thioxo derivatives VIII (3, 4) were obtained from the corresponding thiocarboxamides VII (Scheme 1A, i') without isolating

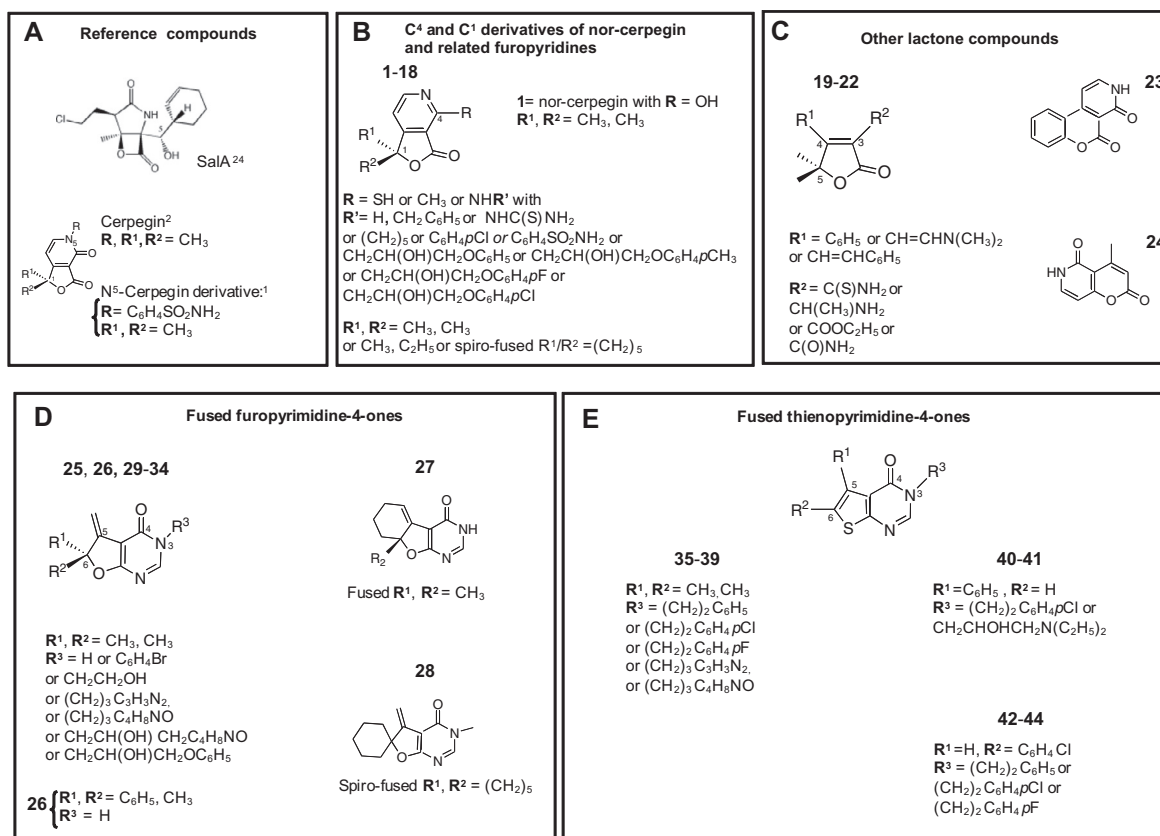


**Figure 1.** General presentation of the C<sup>4</sup> and C<sup>1</sup> derivatives of nor-cerpegin, of related furo-pyrimidines and of fused furo- and thienopyrimidine-4-ones synthesized in this study: (A) General structures of reference compounds are shown: SalA molecule with a  $\beta$ -lactone<sup>24</sup> and cerpegin<sup>2</sup> or a N<sup>5</sup> cerpegin derivative (compound **1** in Ref. 1) with a  $\gamma$ -lactone moiety. (B) C<sup>4</sup> and C<sup>1</sup> derivatives of nor-cerpegin (**1, 2** and **10–18**, series **IV, VI**) and related furo-pyrimidines (**8, 9, 3, 4** and **5, 6**, series **III, VIII** and **XI**); R<sup>1</sup> and R<sup>2</sup> substituents for nor-cerpegin (**1**) are both a methyl group. (C) Other lactones models:  $\gamma$ -lactones (**19–22**) and  $\delta$ -lactones (**23** and **24**). (D) Fused furo-pyrimidine-4-ones: the furan ring is now fused to a pyrimidine ring and the  $\gamma$ -lactone moiety absent but a carbonyl group is present at the C<sup>4</sup> position of the pyrimidine ring (**25–34**). (E) Fused thienopyrimidine-4-ones: the furan ring is now replaced by a thieno ring fused to a pyrimidine ring. A carbonyl group is present at the C<sup>4</sup> position of the pyrimidine ring (**35–44**).

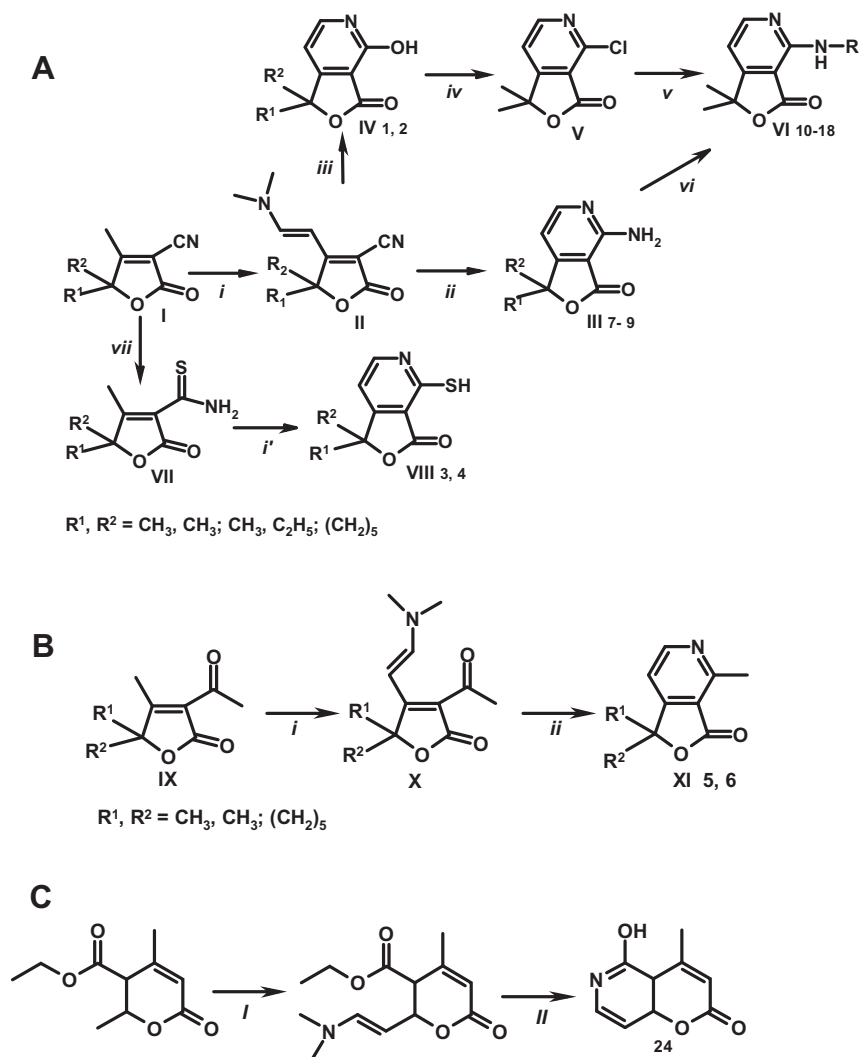
intermediate dimethylaminovinyl derivatives. The initial thiocarboxamides<sup>36</sup> **VII** were obtained from lactones **I**. The 4-methyl-derivatives **XI** (**5, 6**) (Scheme 1B) were obtained from 3-acetyl-furan-2(5H)-one compounds **IX** through the corresponding dimethylaminovinyl intermediates **X** by ring formation in the presence of ammonia.

Model  $\gamma$ -lactones (Fig. 1C) including 5,5-dimethyl-4-phenyl-5H-furan-2-ones **19–20**<sup>35,36</sup> and 4-vinylactones **21**<sup>2, 22</sup>,<sup>37</sup> with various functional groups at C<sup>3</sup> and C<sup>4</sup> were prepared as already described. The condensed pyridine-dione  $\delta$ -lactone **23** (Fig. 1C) was synthesized, starting from 4-methyl-2-oxo-2H-chromene-3-carbonitrile and following steps *i* and *iii* as in Scheme 1A [condensation with DMF DMA in xylene and further cyclization of obtained product in AcOH/HCl (1:3) solution].<sup>38</sup> The condensed pyridine-dione  $\delta$ -lactone **24** was obtained from methyl 2,4-dimethyl-6-oxo-3,6-dihydro-2H-pyran-3-carboxylate as described in Scheme 1C.

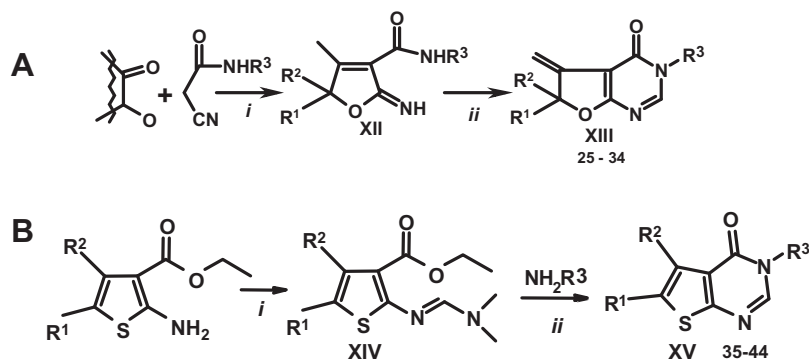
Several new furo[2,3-*d*]pyrimidine-4-ones (**25–31**) (Fig. 1D) and thieno[2,3-*d*]pyrimidine-4-ones **32–38** (Fig. 1E) were obtained via dimethylaminomethyleneamino derivatives through pyrimidine cycle formation. Furo-pyrimidinones were prepared as outlined in Scheme 2A. Starting imino derivatives were synthesized by the reaction of amides of cyanoacetic acid with the corresponding keto-alcohol. Condensation of 2-imino-4,5,5-trisubstituted-2,5-dihydro-furan-3-carboxamides **XII** with DMF DMA yielded the fused compounds **XIII**. Thieno[2,3-*d*]pyrimidine-4-ones **XV** (**35–44**) were synthesized in xylene from Gewald thiophenes (Scheme 2B and Supplemental data).

For each of these compounds, yields and melting points as well as <sup>1</sup>H NMR data are reported in Supplementary section. <sup>13</sup>C NMR and GCMS data are also reported for compounds **3, 7, 8, 10, 15, 18, 24** and **40**.

Tables 1 and 2 show the IC<sub>50</sub> values (concentrations giving 50% inhibition) obtained for each kind of peptidase activity, after incubation of a purified c20S fraction with the respective furo-pyrimidine-3-ones and furo- or thienopyrimidine-4-ones. Assays were conducted following the protocols previously described for each activity<sup>1,2</sup> and summarized in Ref. 39. A similar protocol was used for the i20S purified fraction.<sup>39</sup> The results obtained for the C<sup>4</sup>-substituted furo-pyrimidine-3-ones (**1–18**) and related condensed  $\gamma$ -lactones (**19–22**) or pyridine-fused  $\delta$ -lactones (**23** and **24**) are summarized in Table 1. Compounds **1–18** show replacement of the C<sup>4</sup>-carbonyl group normally present in cerpegin and furo-pyrimidine-3,4-dione derivatives<sup>1,2</sup> by a large diversity of chemical groups. Among them are found: a hydroxyl group in nor-cerpegin (**1**, Fig. 1B) and its analog **2**, a sulfhydryl in **3, 4**, a methyl in **5, 6**, a primary amine in **7–9**, a secondary amine in **10, 11, 13–18** and a tertiary amine in **12**. Compounds **3, 5, 7** and **10–18** were dimethylated at C<sup>1</sup> as is the case for nor-cerpegin (**1**, this study) or for cerpegin.<sup>2</sup> A spiro-cyclohexane-fused group is the C<sup>1</sup> substituent for compounds **2, 4, 6** and **9**. Compound **10**, bearing a benzylamino group at C<sup>4</sup>, strongly inhibited the PA activity of c20S (IC<sub>50</sub><sup>PA</sup> of 600 nM). In the range of 100 to 2000 nM, a selective inhibition of the c20S vs i20S was found (no inhibition detected for the i20S, Table 1). At the whole cell level, compound **10** also inhibited PA activity of HeLa

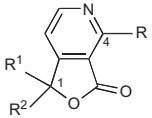
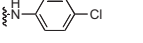
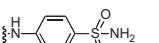
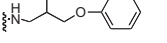
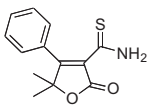
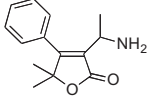
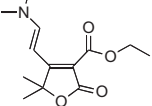


**Scheme 1.** Synthesis of 1,1-dialkyl-1H,5H-furo[3,4-c]pyridine-3-one 4-derivatives **IV** (**1, 2**), **VIII** (**3, 4**), **III** (**7–9**), **VI** (**10–18**) (A), **XI** (**5, 6**) (B) and related pyridinone-fused  $\delta$ -lactone **24** (C). (A) Reagents and conditions: (i) **I**, dimethylformamide dimethylacetal (DMF DMA), xylene, reflux 5 h., 89–96% yield; (i') **VII**, DMF DMA, heating 90 °C, 4 h, yields 72–76%; (ii) **II**, ammonia 20%, reflux 4 h, yields 72–89%; (iii) **II**, AcOH/HCl (3:1), reflux 4 h, yields 94–99%; (iv) **IV** (**1**),  $\text{PCl}_5$ , 130 °C, 15–20 min; (v) a) **V**,  $\text{NH}_2\text{R}$  1:5 molar ratio, xylene, reflux 2.5 h, b) **V**,  $\text{NHR}_2$ , 1:33 molar ratio, DMF, reflux 2.5 h, yield 74%; c) **V**,  $\text{NH}_2\text{Ar}$  1:1 molar ratio, AcOH, reflux 10 h, yield 58–68%; (vi) **III** (**7**), 2-phenoxymethyloxirane, 2–3 drops of water, isopropyl alcohol, reflux 20 h., yields 51–55%; (vii) **I**,  $\text{H}_2\text{S}$ , benzene,  $\text{Et}_3\text{N}$ , 2 h. (B) Reagents and conditions: (i) **IX**, DMF DMA, xylene, reflux 3.5 h., 83–96% yield; (ii) **X**, ammonia 20%, reflux 5 h, yields 75–83%. (C) Reagents and conditions: (i) commercially available 2,4-dimethyl-6-oxo-3,6-dihydro-2H-pyran-3-carboxylate, DMF DMA, xylene, reflux 5 h; (ii) obtained product, 20% ammonia, reflux 4 h.



**Scheme 2.** Synthesis of 1,1-dialkyl-5-methylene-5,6-dihydro-3H-furo[2,3-d]pyrimidine-4-ones **XIII** (A) and of 3-substitutedthieno[2,3-d]pyrimidine-4(3H)-one **XV** **35–44** (B) (A) Reagents and conditions: (i) amid of cyano-acetic acid, corresponding carbinol, ethyl alcohol, Sodium ethylate, room temperature, 24 h; (ii) **XII**, DMF DMA (1:1.2 molar ratio), benzene/DMF, reflux 5 h, 52–78% yield. (B) Reagents and conditions: (i) ethyl 2-aminothiophene-3-carboxylate, DMF DMA (1:1), xylene, reflux 7 h; (ii) ethyl 2-(dimethylaminomethyleneamino)-thiophene-3-carboxylate **XIV** and  $\text{NH}_2\text{R}$  1:3 molar ratio, xylene, reflux 35 h.

**Table 1**Inhibition of mammalian proteasomes by 4-R-1,1-disubstituted-1*H*,5*H*-furo[3,4-*c*]pyridine-3-ones (compounds **1–18**, series **III**, **IV**, **VI**, **VIII**, **XI**) and by model compounds:  $\gamma$ - (**19–22**) and pyridone-fused  $\delta$ -lactones (**23**, **24**)

Compound			IC <sub>50</sub> ( $\mu$ M) or % inhibition at 100 $\mu$ M			
	R	Separate R <sup>1</sup> , R <sup>2</sup> or spiro-fused R <sup>1</sup> /R <sup>2</sup>	CT-L	T-L	PA	
<b>1</b>		$\frac{5}{2}$	$\frac{5}{2}$	ni	ni	16.7 $\pm$ 1.0
<b>2</b>			$\frac{5}{2}$	ni	ni	27.8 $\pm$ 2.0
<b>3</b>		$\frac{5}{2}$	$\frac{5}{2}$	79 $\pm$ 6	ni	(48%)
<b>4</b>			$\frac{5}{2}$	(52%)	ni	(20%)
<b>5</b>		$\frac{5}{2}$	$\frac{5}{2}$	ni	88 $\pm$ 12	ni
<b>6</b>			$\frac{5}{2}$	ni	ni	16.1 $\pm$ 0.8
<b>7</b>		$\frac{5}{2}$	$\frac{5}{2}$	ni	(35%)	7.9 $\pm$ 0.3
<b>8</b>		$\frac{5}{2}$	$\frac{5}{2}$	(21.5%)	ni	7.0 $\pm$ 0.2
<b>9</b>			$\frac{5}{2}$	ni	ni	8.4 $\pm$ 0.5
<b>10</b>		$\frac{5}{2}$	$\frac{5}{2}$	ni	ni	0.60 $\pm$ 0.02 *ni at 2 $\mu$ M
<b>11</b>		$\frac{5}{2}$	$\frac{5}{2}$	(26%)	(29%)	(41%)
<b>12</b>		$\frac{5}{2}$	$\frac{5}{2}$	ni	ni	(41.6%)
<b>13</b>		$\frac{5}{2}$	$\frac{5}{2}$	(24.5%)	ni	(41.5%)
<b>14</b>		$\frac{5}{2}$	$\frac{5}{2}$	ni	ni	ni at 25 $\mu$ M
<b>15</b>		$\frac{5}{2}$	$\frac{5}{2}$	ni	ni	48.1 $\pm$ 0.7
<b>16</b>		$\frac{5}{2}$	$\frac{5}{2}$	(36.5%)	60.8 $\pm$ 9.6	ni
<b>18</b>		$\frac{5}{2}$	$\frac{5}{2}$	(29%)	ni	ni
<b>18</b>		$\frac{5}{2}$	$\frac{5}{2}$	(63%)	48.1 $\pm$ 2.7	ni
<i>Other lactone-containing compounds</i>						
<b>19</b> <sup>35,36</sup>				ni	ni	ni
<b>20</b> <sup>35,36</sup>				ni	ni	ni
<b>21</b> <sup>2</sup>				ni	ni	ni

(continued on next page)

Table 1 (continued)

Compound		IC <sub>50</sub> (μM) or % inhibition at 100 μM		
		CT-L	T-L	PA
22 <sup>37</sup>		ni	ni	ni
23 <sup>38</sup>		ni	ni	ni
24		29.4 ± 1.8	8.7 ± 0.8	ni
Cerpegin <sup>2</sup>		ni	ni	10.4 ± 0.5
Cerpegin N <sup>5</sup> -derivative <sup>1</sup>		ni	ni	6.1 ± 0.3 <sup>a</sup>
SalA <sup>24</sup>		0.0026	0.021	0.46

Inhibition of constitutive proteasome (c20S) from rabbit erythrocytes is expressed as IC<sub>50</sub> values or as % inhibition at 100 μM (italics between parentheses). Inhibition of immunoproteasome (i20S) from human blood monocytes is given for compound **10** and labeled with an asterisk\*. ni = no inhibition. Cerpegin<sup>2</sup>, a N<sup>5</sup> derivative of cerpegin<sup>1</sup> and Salinosporamide A (SalA)<sup>24</sup> are given as reference inhibitors.

<sup>a</sup> IC<sub>50</sub> values for compound **1** in Ref. 1.

Table 2

Inhibition of mammalian proteasomes by furo[2,3-*d*]pyrimidines (**25–34**, series **XIII**) and thieno[2,3-*d*]pyrimidines (**35–44**), series **XV** derivatives

Compound	Furo- and Thieno[2,3- <i>d</i> ]pyrimidine-4-ones	IC <sub>50</sub> (μM) or % inhibition at 100 μM		
		CT-L	T-L	PA
25		ni	59 ± 5	ni
26		ni	ni	ni
27		ni	ni	ni
28		(30%)	ni	ni
29		ni	(29%)	ni
30		ni	ni	ni
31		ni	(56%)	47 ± 1.6
32		ni	(48%)	ni
33		(33%)	ni	ni
34		ni	ni	ni

Table 2 (continued)

Compound	Furo- and Thieno[2,3-d]pyrimidine-4-ones	IC <sub>50</sub> (μM) or % inhibition at 100 μM		
		CT-L	T-L	PA
35		ni	(42%)	ni
36		ni	56 ± 1.3	ni
37		ni	ni	ni
38		ni	42% at 50 μM	ni
39		ni	(53%)	ni
40		ni	9.9 ± 0.4 *6.7 ± 0.6	ni
41		36% at 50 μM	19.4 ± 1.9	25% at 50 μM
42		ni	(48%)	ni
43		ni	(52%)	ni
44		ni	56% at 50 μM	ni

Inhibition of constitutive 20S proteasome from rabbit erythrocytes is expressed as IC<sub>50</sub> values or as % inhibition at 100 μM (italics between parentheses). For some compounds, % inhibition was tested at 50 μM. Inhibition of immunoproteasome (i20S) from human blood monocytes is given for compound **40** and labeled with an asterisk\*. ni = no inhibition.

cervical cancer cell line (IC<sub>50</sub><sup>PA</sup> cel = 11.6 ± 0.6 μM). At these concentrations no cytotoxicity was found. Only higher concentrations were found to be mildly cytotoxic (35% inhibition of mitochondrial dehydrogenase activity at 50 μM) and to decrease cell attachment. Further analysis is necessary to determine this negative cellular effect of compound **10** more precisely.

Compound **14**, with a 4-benzenesulfonamide substituent at C<sup>4</sup> did not inhibit PA activity at high concentration (25 μM), in contrast with the N<sup>5</sup>-substituted analogous compound (Table 1, reference compound **1**<sup>1</sup>) which exerted submicromolar inhibition (IC<sub>50</sub><sup>CPA</sup> of 6 μM). In the same manner compound **15**, with a 4-(2-hydroxy-3-phenoxy propylamino) group at C<sup>4</sup>, exerted very low inhibition of PA (IC<sub>50</sub><sup>CPA</sup> of 48 μM). Similar results were obtained with the analogous substitution at N<sup>5</sup>.<sup>1</sup> When the above-mentioned phenoxy propylamino group was declined with diverse substitutions in *para*-position of the phenyl ring (-methyl in **16**, -fluoro in **17** or -chloro in **18**) PA inhibition was no longer detected. A slight

inhibition of T-L activity could be noted for **16** and **18** (IC<sub>50</sub><sup>CT-L</sup> of 61 μM and 48 μM, respectively).

Remarkably, in this C<sup>4</sup>-substituted series of compounds derived from nor-cerpegin (**1–18**), an optimization of the inhibition potency of PA activity was found for compound **10**. Moreover, neither this C<sup>4</sup> benzylamino substituent in compound **10** nor other C<sup>4</sup> substituents allow inhibition of the two other proteolytic sites with the exception of **16** and **18** for which the T-L activity was slightly inhibited. This was consistent with the previously reported absence of inhibition caused by the analogous N<sup>5</sup>-substituted compounds derived from cerpegin<sup>1</sup> which selectively inhibited the PA activity of c20S.

In the series of model compounds with related γ-lactones (**19–22**) or pyridinone-fused δ-lactones (**23–24**) (Fig. 1C and Table 1), no inhibition of the three proteolytic activities was found for compounds **19–22**, ruling out the possibility that the pyridine ring of the fused furo-pyridine-3-one structure could participate in PA

inhibition. Compound **24** behaved differently in that it inhibited CT-L and T-L mildly but not PA activity ( $IC_{50}^{CT-L}$  of 29  $\mu$ M and 9  $\mu$ M, respectively).

None of the compounds studied in this series (**1–24**) worked on fractions of cathepsin B or calpain I.

Results for the assays with furo- or thienopyrimidine-4-ones are summarized in Table 2.

All the compounds studied with a fused furo-pyrimidine ring bear a carbonyl at C<sup>4</sup> of the fused ring (**25–34**, Fig. 1D, Table 2). With the exception of **25** and **31**, which exerted mild inhibition of T-L and PA activities, respectively, none of these compounds were inhibitors of c20S. Compounds with a fused thienopyrimidine ring (**35–44**, Fig. 1E, Table 2) also bear a carbonyl group at C<sup>4</sup> of the fused ring. In this series, no inhibition of the PA or CT-L activities was observed. However, mild inhibition of the T-L activity was noted for compounds **36**, **40** and **41** ( $IC_{50}^{CT-L}$  of 56  $\mu$ M, 10  $\mu$ M and 19  $\mu$ M, respectively). The T-L inhibition of i20S by **40** confirmed the efficiency of this compound ( $IC_{50}^{T-L}$  of 7  $\mu$ M).

To summarize, in the series of furo-pyridine-3-ones, only the  $\gamma$ -lactone compounds fused to a pyridine ring substituted at C<sup>4</sup> were found to inhibit PA activity specifically in the c20S. The SH group at C<sup>4</sup> was inefficient as compared to the OH and NH<sub>2</sub> groups at the same position. Compound **10** with a C<sup>4</sup>-substituted benzylamino group was the most potent inhibitor, working specifically on the constitutive PA activity at the nanomolar range. For this activity, cerpegin  $\gamma$ -lactone<sup>2</sup> and such an N<sup>5</sup> derivative as compound **1** in Ref. 1 (Table 1) were seventeen and ten times less efficient, respectively. Although SaLa  $\beta$ -lactone is a better inhibitor of CT-L and T-L activities<sup>24</sup>, it is worth noting that the  $IC_{50}$  value of **10** observed

here for cPA is not very different from that reported for SaLa on the same activity (Table 1<sup>24</sup>). In the series of furo- and thienopyrimidine-4-ones, compound **40** specifically inhibited T-L activity of c20S or i20S, although at micromolar concentrations.

The binding mechanisms of compound **10** to the PA active sites were studied performing in silico docking experiments (Fig. 2). Catalytic  $\beta$ 1 chains used as targets were from the constitutive mouse 20S proteasome<sup>7</sup> (*Mm* $\beta$ 1c, PDB ID: 3UNE, Fig. 2A) and from the mouse immunoproteasome<sup>7</sup> (*Mm* $\beta$ 1i, PDB ID: 3UNH Fig. 2B). For comparison, we also included results obtained with  $\beta$ 1 chains from constitutive bovine 20S proteasome<sup>40</sup> (*Bt* $\beta$ 1c, PDB ID: 1IRU, Fig. 2C) that have been used as target in our previous work for analogous furo-pyridones. All crystal structures were obtained from the protein data bank.<sup>41</sup> These mammalian models were retained due to the very strong amino acid sequence identity between human, mouse and bovine  $\beta$ -type subunits.<sup>42</sup> For example, the bovine  $\beta$ 1 precursor protein is 95% identical to the human one and the identity reaches 98.5% when considering only the mature subunit. In addition, the few non-identical residues are located at the interfaces of  $\beta$ 1 with its neighbors. The specificities of mouse immunoproteasome amino acid sequence have been described and crystallographic data are available for mouse.<sup>7</sup>

The AutoDock Vina program<sup>43</sup> was used for docking calculations,<sup>44</sup> with default parameters. In cases where asymmetric carbons were present, all corresponding configurations were docked.

Visual Molecular Dynamics (VMD)<sup>45</sup> was used to prepare molecular pictures.

The lowest energy (first rank) poses adopted by the C<sup>4</sup>-substituted furo-pyridine **10** in the  $\beta$ 1 catalytic sites of constitutive 20S proteasomes (*Mm* $\beta$ 1c, Fig. 2A and *Bt* $\beta$ 1c, Fig. 2C) were similar to those already described for N<sup>5</sup>- and C<sup>1</sup>-substituted furo-pyridinones in the bovine *Bt* $\beta$ 1c site.<sup>1</sup> The bicyclic furo-pyridine ring fitted into a slit in the active site between Thr residues 1 and 21 (Fig. 2A and C), and the C<sup>3</sup> carbonyl group of the furan ring was positioned at a distance (4.2 Å) compatible with a nucleophilic attack by the O $\gamma$  of Thr1 (red dashed arrow in Fig. 2D). As previously observed for the N<sup>5</sup> substituent,<sup>2</sup> the free end of the C<sup>4</sup> substituent was close to the aromatic ring of Tyr114 of the  $\beta$ 2c subunit. On the contrary, when **10** was docked in the mouse *Mm* $\beta$ 1i chain (Fig. 2B), the first rank pose was different: the 4-benzylamino substituent was seen to enter the S1 specificity pocket and the  $\gamma$ -lactone ring was largely displaced, pointing towards His114 of  $\beta$ 2i. In this case, no relevant interaction was observed between the inhibitor and the Thr1 nucleophile. This correlates with the fact that no inhibition was exerted by compound **10** on the PA active site of the immune human proteasome (Table 1). These observations strengthen the idea already expressed<sup>1,2</sup> that Tyr114 in  $\beta$ 2c could play an important part in the specificity of binding to the PA active site.

In this series of C<sup>4</sup>-substituted furo-pyridines, an 80-fold less efficient compound (**15**) was also docked in *Mm* $\beta$ 1c and *Bt* $\beta$ 1c sites for comparison (Figs. S1 A and C) as well as in *Mm* $\beta$ 1i site (Fig. S1 B). For  $\beta$ 1c sites, these assays revealed an orientation of the fused furo-pyridine ring compatible with the same type of nucleophilic attack as the one suggested for **10** in the same  $\beta$ 1c sites, but the fourth-rank pose did not correspond to the lowest energy one. Furthermore, a different orientation was observed for the C<sup>4</sup> substituent, the phenoxy ring of which deeply entered the S1 specificity pocket. This highlights the importance of the ligand interaction with Tyr114 in the  $\beta$ 2c subunit for the inhibition efficiency on the  $\beta$ 1c catalytic site.

Whatever the enzymatic activity concerned, the necessary prerequisite for inhibition is ligand binding. In terms of binding, our molecules may be compared with HU derivatives described by Gallastegui et al.<sup>29</sup> which non-covalently inhibit CT-L activity in the yeast proteasome. The binding mode predicted for our molecules converges with a novel one described by crystallography

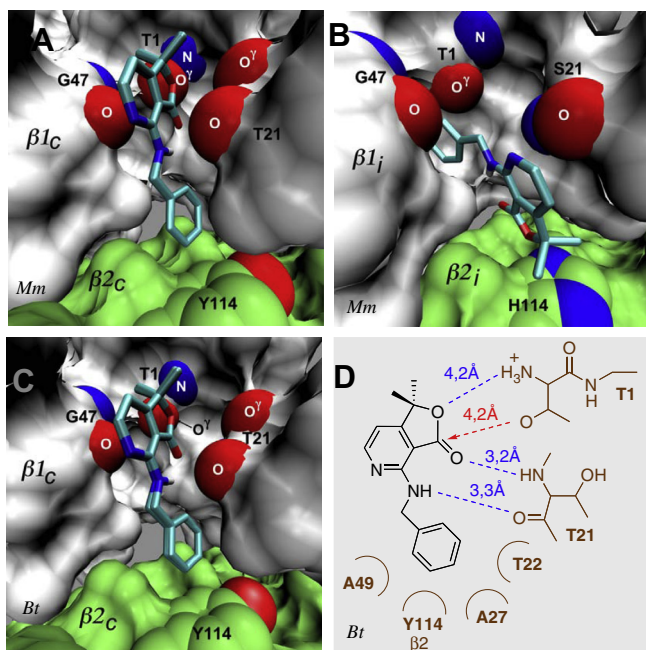


**Figure 2.** In silico docking of compound **10** in the PA active site of mouse (A, B) and bovine (C, D) 20S proteasomes. (A) Mouse constitutive PA site (*Mm* $\beta$ 1c and neighboring *Mm* $\beta$ 2c subunits) (B) Mouse immunoproteasome PA site (*Mm* $\beta$ 1i and neighboring *Mm* $\beta$ 2i subunits) (C) Bovine constitutive PA site (*Bt* $\beta$ 1c and neighboring *Bt* $\beta$ 2c subunits). Protein chains in A, B and C are shown as solvent accessible surfaces and the residues and atoms relevant to an enzyme activity are labeled and colored according to CPK convention. Compound **10** is displayed as stick model colored by atom type. Each docking mode is shown as 6 superimposed poses from the most populated and lowest energy cluster. (D) Distance map corresponding to Figure 2C. Distances between the bovine  $\beta$ 1c subunit and atoms in compound **10** were taken from the lowest energy pose. Putative hydrogen bonds are shown as blue dashed lines and the predicted nucleophilic attack on the lactone carbon, by a dashed red arrow.

for HU derivatives. All these molecules are rather small, non-peptidic and share a clear separation of hydrophobic and hydrophilic moieties. Their hydrophilic heads are pinched between Thr21 and Gly47 and form hydrogen bonds with the main chain atoms of these residues at the entrance of the S1 subsite. Their hydrophobic tails engage in the S3 subsite, contributed in part by the neighboring subunits ( $\beta 2c$  for PA sites and  $\beta 6$  for CT-L sites). In addition, the specificity of HU derivatives towards  $\beta 5$  is due to the presence in these derivatives of a short hydrophobic branch that interacts with residues in the S1 specificity pocket. The non-covalent nature of the catalysis mechanism provided by HU derivatives is correlated with their lack of interaction with the catalytic residue Thr1,<sup>29</sup> whereas docking predicts such interactions for compound **10** of this study (Fig. 2D).

In silico docking suggests that the absence of inhibition of the  $\beta 1i$  activity by **10** is accompanied with an inversion of this binding mode relative to  $\beta 1c$  (Fig. 2A and C), with the hydrophilic head facing the S3 subsite and the hydrophobic tail entering the slightly more hydrophobic S1 subsite (Fig. 2B).

The absence of inhibition of T-L activity by **10** is to be related to its mode of binding to the  $\beta 2$  constitutive active site. Indeed, the first rank pose obtained in the  $\beta 2c$  active site of the bovine proteasome (Fig. 3A) was almost identical to the one observed in the mouse  $\beta 1i$  site with the 4-benzylamino substituent deeply engaged into the S1 specificity subsite and the furopyridine ring pointing toward Asp125, which occupies in  $\beta 3$  the same spatial position as His114 in  $\beta 2i$ . This comparison gives support to the selective inhibition of constitutive PA activity by **10**. More canonical binding modes of compound **18** to the  $\beta 2c$  catalytic site are illustrated in Fig. 3B. The position of the molecule remained compatible with the nucleophilic attack of the  $\gamma$ -lactone by Thr1 but the rank of

the pose was very bad (8–10), in relation with the poor efficiency of the compound in T-L inhibition ( $IC_{50}$  of 48  $\mu M$ ).

Promising inhibitions of both constitutive and immuno T-L activities were obtained after incubation with the thienopyrimidine-4-one **40** ( $IC_{50}^{T-L}$  9.9  $\mu M$  and 6.7  $\mu M$ , respectively, Table 2). The catalytic  $\beta 2$  chains from the mouse 20S proteasomes (*Mm* $\beta 2c$ , Fig. 3C and *Mm* $\beta 2i$ , Fig. 3D) were then used as targets for docking experiments. Accordingly, docking revealed almost identical first rank poses of **40** in the two active sites with the *para*-chlorophenethyl substituent engaged in the S1 specificity pocket (Fig. 3C and D). Beyond this, we found no pose suggesting the possibility of a nucleophilic attack of this molecule by Thr1.

In conclusion, our results highlight the functional importance of a  $\gamma$ -lactone fused to pyridine ring in the selectivity of PA inhibition. Indeed, compound **10** from the furopyridine-3-one family specifically targeted the constitutive PA sites. Comparison of this result with the results previously reported with furopyridine-3,4-diones<sup>1,2</sup> show an optimization of 20S proteasome inhibition when the C<sup>4</sup> carbonyl is replaced by a benzylamino group. In spite of this optimization, docking analysis suggests a unique mode of binding with the C<sup>3</sup> carbonyl of the furan ring positioned at a distance compatible with a nucleophilic attack by the O $\gamma$  of Thr1. This further suggests that the optimization noted above is not related to different positions of the molecules in the active site but, rather, to the details of intermolecular interactions. In contrast, in the thieno[2,3-*d*]pyrimidine-4-one family of compounds, that is, in the absence of the typical furopyridine-3-one ring, PA activities were not inhibited. Moreover, in compound **40** of the same family, T-L activities were specifically reduced at the micromolar range in both the constitutive proteasome and its immunoisform.

## Acknowledgments

A.H., A.P., G.M. received financial supports from the Yerevan University (A.H., A.P., G.M.) and from a Grant of the State Committee Science MES RA, in frame of the research project No. SCS 13-1D330 (A.H., G.M.). T.H.P. received financial supports from the Vietnamese Ministry for Education (T.H.P.). M.B.D., M.R.R., D.B., L.D., L.Q. and Y.C. received supports from the Pierre et Marie Curie University (UPMC, Paris 6) and from a Grant of the 'French Association against myopathies'.

## Supplementary data

Supplementary data associated with this article can be found, in the online version, at <http://dx.doi.org/10.1016/j.bmcl.2014.01.072>.

## References and notes

- Hovhannisyanyan, A.; Pham, T. H.; Bouvier, D.; Qin, L. X.; Melikyan, G.; Reboud-Ravaux, M.; Bouvier-Durand, M. *Bioorg. Med. Chem. Lett.* **2013**, *23*, 2696.
- Pham, T. H.; Hovhannisyanyan, A.; Bouvier, D.; Tian, L.; Reboud-Ravaux, M.; Melikyan, G.; Bouvier-Durand, M. *Bioorg. Med. Chem. Lett.* **2012**, *22*, 3822.
- Crawert, M. A.; Groll, M. *Chem. Commun. (Camb)* **2012**, *48*, 1364.
- Kisselev, A. F.; van der Linden, W. A.; Overkleeft, H. S. *Chem. Biol.* **2012**, *19*, 99.
- Genin, E.; Reboud-Ravaux, M.; Vidal, J. *Curr. Top. Med. Chem.* **2010**, *10*, 232.
- Stein, M. L.; Groll, M. *BBA*, **2013**, in press.
- Huber, E. M.; Basler, M.; Schwab, R.; Heinemayer, W.; Kirk, C. J.; Groettrup, M.; Groll, M. *Cell* **2012**, *148*, 727.
- King, R. W.; Deshaies, R. J.; Peters, J. M.; Kirschner, M. W. *Science* **1996**, *274*, 1652.
- Friedman, J.; Xue, D. *Dev. Cell* **2004**, *7*, 460.
- Konstantinova, I. M.; Tsmokha, A. S.; Mittenberg, A. G. *Int. Rev. Cell Mol. Biol.* **2008**, *267*, 59.
- Vembar, S. S.; Brodsky, J. L. *Nature Rev. Mol. Cell Biol. (Camb)* **2008**, *9*, 944.
- Rock, K. L.; Goldberg, A. L. *Annu. Rev. Immunol.* **1999**, *17*, 739.
- Coux, O.; Tanaka, K.; Goldberg, A. L. *Ann. Rev. Biochem.* **1996**, *65*, 801.
- Hershko, A.; Ciechanover, A. *Ann. Rev. Biochem.* **1998**, *67*, 425.
- Borissenko, L.; Groll, M. *Chem. Rev.* **2007**, *107*, 687.

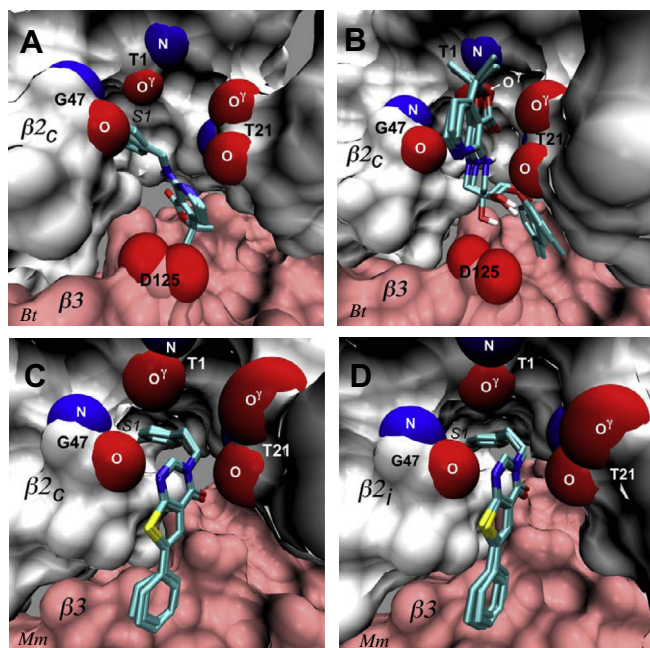


**Figure 3.** In silico docking of compounds **10** (A), **18** (B) and **40** (C, D) in the T-L active site of diverse 20S proteasomes. (A) Compound **10** in the bovine constitutive T-L site (*Bt* $\beta 2c$  and neighboring *Bt* $\beta 3$  subunits). (B) Compound **18** in the bovine constitutive T-L site (*Bt* $\beta 2c$  and neighboring *Bt* $\beta 3$  subunits). (C) Compound **40** in the mouse constitutive T-L site (*Mm* $\beta 2c$  and neighboring *Mm* $\beta 3$  subunits). (D) Compound **40** in the mouse T-L site (*Mm* $\beta 2i$  and neighboring *Mm* $\beta 3$  subunits). Protein chains are shown as solvent accessible surfaces and the residues and atoms relevant to an enzyme activity are labelled and colored according to CPK convention. Compounds are displayed as stick model colored by atom type. Each docking mode is shown as 3 (A) or 6 (B) superimposed poses (see text for details). For compound **18**, the reported configuration of the hydroxyl is S.

16. Marques, A. J.; Palanimurugan, R.; Matias, A. C.; Ramos, P. C.; Dohmen, R. J. *Chem. Rev.* **2009**, *109*, 1509.
17. Weissman, A. M.; Shabek, N.; Ciechanover, A. *Nat. Rev. Mol. Cell Biol.* **2011**, *12*, 605.
18. Muchamuel, T.; Basler, M.; Aujay, M. A.; Suzuki, E.; Kalim, K. W.; Lauer, C.; Sylvain, C.; Ring, E. R.; Shields, J.; Jiang, J., et al. *Nat. Med.* **2009**, *15*, 781.
19. Kuhn, D. J.; Orłowski, R. Z.; Bjorklund, C. C. *Curr. Cancer Drug Targets* **2011**, *11*, 285.
20. Myung, J.; Kim, K. B.; Lindsten, K.; Dantuma, N. P.; Crews, C. M. *Mol. Cell* **2001**, *7*, 411.
21. Britton, M.; Lucas, M. M.; Downey, S. L.; Screen, M.; Pletnev, A. A.; Verdoes, M.; Tokhunts, R. A.; Amir, O.; Goddard, A. L.; Pelphrey, P. M., et al. *Chem. Biol.* **2009**, *16*, 1278.
22. van der Linden, W. A.; Willems, L. I.; Shabaneh, T. B.; Li, N.; Ruben, M.; Florea, B. I.; van der Marel, G. A.; Kaiser, M.; Kisselev, A. F.; Overkleef, H. S. *Org. Biomol. Chem.* **2012**, *10*, 18.
23. Mirabella, A. C.; Pletnev, A. A.; Downey, S. L.; Florea, B. I.; Shabaneh, T. B.; Britton, M.; Verdoes, M.; Filippov, D. V.; Overkleef, H. S.; Kisselev, A. F. *Chem. Biol.* **2011**, *18*, 608.
24. Macherla, V. R.; Mitchell, S. S.; Manam, R. R.; Reed, K. A.; Chao, T. H.; Nicholson, B.; Deyanat-Yadzi, G.; Mai, B.; Jensen, P. R.; Fenical, W. F.; Neuteboom, S. T. C.; Lam, K. S.; Palladino, M. A.; Potts, B. C. M. *J. Med. Chem.* **2005**, *48*, 3684.
25. Lawasut, P.; Chauhan, D.; Laubach, J.; Hayes, C.; Fabre, C.; Maglio, M.; Mitsiades, C.; Hideshima, T.; Anderson, K. C.; Richardson, P. G. *Curr. Hematol. Malig. Rep.* **2012**, *7*, 258.
26. Kisselev, A. F.; Goldberg, A. L. *Chem. Biol.* **2001**, *8*, 739.
27. Zhang, S.; Shi, Y., et al. *J. Mol. Model.* **2009**, *15*, 1481.
28. Beck, P.; Dubiella, C.; Groll, M. *Biol. Chem.* **2012**, *393*(10), 1101.
29. Gallastegui, N.; Beck, P.; Arciniega, M.; Huber, R.; Hillebrand, S.; Groll, M. *J. Mol. Graphics* **2012**, *51*, 42. *Angew. Chem., Int. Ed.*, *51*, 247.
30. Maréchal, X.; Genin, E.; Qin, L.; Sperandio, O.; Montes, M.; Basse, N.; Richey, N.; Miteva, M. A.; Reboud-Ravaux, M.; Vidal, J.; Villoutreix, B. O. *Curr. Med. Chem.* **2013**, *20*, 2351.
31. Groll, M.; Goetz, M.; Kaiser, M.; Weyher, E.; Moroder, L. *Chem. Biol.* **2006**, *13*, 607.
32. Blackburn, C.; Gigstad, K. M.; Hales, P.; Garcia, K. M.; Barrett, M.; Liu, J. X.; Soucy, T. A.; Sappal, D. S.; Bump, N.; Olhava, E. J.; Fleming, P.; Dick, L. R.; Tsu, C.; Sintchak, M. D.; Blank, J. L. *Biochem. J.* **2010**, *430*, 461.
33. Groll, M.; Gallastegui, N.; Maréchal, X.; Le Ravalec, V.; Basse, N.; Richey, N.; Genin, E.; Huber, R.; Moroder, L.; Vidal, J.; Reboud-Ravaux, M. *ChemMedChem* **2010**, *1701*.
34. Desvergne, A.; Genin, E.; Maréchal, X.; Gallastegui, N.; Dufau, L.; Richey, N.; Groll, M.; Vidal, J.; Reboud-Ravaux, M. *J. Med. Chem.* **2013**, *56*, 3367.
35. Communication by Melikyan, G., Hovhannisyanyan, A. and Avetisyan, A. at the Congress of the French Chemical Society «La Chimie du Futur. Le Futur de la Chimie» SFC 07, Paris, July 16–18 2007.
36. (a) Avetisyan, A.A.; Melikyan, G.S.; Danghian, M.T., The inventor's certificate, USSR, N 424425 (11.11.1971); (b) Knott, E. B. *J. Chem. Soc.* **1948**, 186.
37. Perjessy, A.; Avetisyan, A. A.; Akhnazarian, A. A.; Melikyan, G. S. *Chem. Commun.* **1989**, *54*, 1666.
38. Mandal, T. K.; Kuznetsov, V. V.; Soldatenkov, A. T. *Chem. Heterocycl. Compd.* **1994**, *30*, 867.
39. (a) In vitro measurements of CT-L, T-L and PA activities of the constitutive proteasome were realized as previously described in Ref. 1,2 mainly using c20S fractions from rabbit erythrocytes and the respective synthetic substrates Suc-LLVY-AMC, Boc-LRR-AMC and Z-LLE-βNA. In some cases, human erythrocytes c20S fractions were used. In summary, after a pre-incubation period of 15 min with the enzyme ( $[E_0] = 0.27 \text{ nM}$ ) in the absence (control) or presence of test compounds (0.1–100 μM), reactions started after addition of the respective substrates ( $[S_0] = 50 \text{ μM}$  for CT-L and ( $[S_0] = 100 \text{ μM}$  for PA and T-L activities) and were followed for 45 min at 37 °C. The buffers (pH 7.5) were 20 mM Tris, 1 mM DTT, 10% glycerol, 0.02% (w/v) SDS for CT-L and PA activities, and 20 μM Tris, 1 mM DTT, 10% glycerol for T-L activity. In vitro measurements of iPA and iT-L activities were realized using i20S fractions from human erythrocytes and the buffers described above for the homologous PA and T-L activities. A 2-min pre-incubation period was used for each activity and initial concentrations for the respective Z-LLE-βNA and Boc-LRR-AMC substrates were as follows:  $[S_0] = 50 \text{ μM}$  and  $100 \text{ μM}$ , respectively. In vitro measurements of calpain I and cathepsin B activities were realized using human fractions and the respective Suc-LLVY-AMC and Z-RR-AMC substrates. Buffers and temperatures used were: 50 mM Tris, 100 μM CaCl<sub>2</sub> and 10 mM DTT (pH 7.2) at 25 °C for calpain I, and 352 mM KH<sub>2</sub>PO<sub>4</sub>, 48 mM Na<sub>2</sub>HPO<sub>4</sub>, 1 mM EDTA, 1 mM DTT (pH 6) at 37 °C for cathepsin B. In all enzymatic assays, emitted fluorescence was measured using black 96-well microplates and a BMG Fluostar microplate reader. The inhibitor concentrations giving 50% inhibition (IC<sub>50</sub> values) were obtained by plotting the percent inhibition against inhibitor concentration to equation: % inhibition =  $100[I]/(IC_{50}^{nH} + [I]^{nH})$ , or equation: % inhibition =  $100[I]^{nH}/((IC_{50}^{nH} + [I]^{nH})$  where nH is the Hill number.; (b) In vivo measurements of the PA activity in HeLa cervical cancer cell line were conducted with the proteasome cell-based assay from Promega. HeLa cells were incubated in DMEM medium supplemented with the inhibitor for 17 h at 37 °C. White 96-well microplates were seeded with 5000 cells in 100 μL DMEM per well. Control assays were made in the same conditions, without inhibitor. A second step of incubation was realized at 20 °C for 1 h in order to place cells at the optimum temperature for the reactions to reveal proteasomal activity. Measurements of intracellular PA activity were done by adding a 1:1 (vol/vol) mixture of the PA-substrate Z-nLpNLd conjugated to aminoluciferine and luciferase to the cells. Chemiluminescence measurements were done after 5-min reaction using a BMG Fluostar microplate reader. In-cell IC<sub>50</sub> values (IC<sub>50</sub> cel) were calculated as described above.; (c) Cytotoxicity assays were conducted using the reduction capacities of mitochondrial dehydrogenases from living cells to turn a colorless tetrazolium salt solution (XTT from Sigma) into an orange solution of formazan. HeLa cells were prepared as described for measurements of in-cell proteasomal activities and incubation periods with inhibitor were of 18 or 72 h. Readings were made by spectrophotometry at 485 nm after a 3-h period of reaction with a 1 mg/mL XTT solution.
40. Unno, M.; Mizushima, T.; Morimoto, Y.; Tomisugi, Y.; Tanaka, K.; Yasuoka, N.; Tsukihara, T. *Structure* **2002**, *10*, 609.
41. Berman, H. M.; Westbrook, J.; Feng, Z.; Gilliland, G.; Bhat, T. N.; Weissig, H.; Shindyalov, I. N.; Bourne, P. E. *Nucleic Acids Res.* **2000**, *28*, 235.
42. UniProt Consortium *Nucleic Acids Res.* **2012**, *40*, D71.
43. Trott, O.; Olson, A. J. *J. Comput. Chem.* **2010**, *31*, 455.
44. The docking space was limited to a 20 × 20 × 20 Å box centered on the N terminal threonine of the catalytic subunits. Docking modes were selected on the basis of the distance (3–4 Å) between the carbonyl carbon of the compound lactone and the hydroxyl oxygen of the N terminal threonine of each subunit.
45. Humphrey, W.; Dalke, A.; Schulten, K. *J. Mol. Graphics* **1996**, *14*, 33.